Article

Reproducibility of the Hydrodynamic Performance and Measurements in a Liquid–Liquid Kühni Extraction ColumnRelevance to Theoretical Model Evaluation

Lusa N. Gomes, Margarida L. Guimares, Jos C. Lopes, Carlos N. Madureira, Johann Stichlmair, and Jos J. Cruz-Pinto

Ind. Eng. Chem. Res., **2004**, 43 (4), 1061-1070 • DOI: 10.1021/ie030277i

Reproducibility of the Hydrodynamic Performance and Measurements in a Liquid−Liquid Kühni Extraction Column−Relevance to Theoretical Model Evaluation

Luísa N. Gomes,[†] Margarida L. Guimarães,[†] José C. Lopes,[†] Carlos N. Madureira,[‡] Johann Stichlmair,[§] and José J. Cruz-Pinto*[,||]

CIEA/Departamento de Engenharia Química and Faculdade de Engenharia, Instituto Superior de Engenharia do Porto, Porto, Portugal, Lehrstuhl für Fluidverfahrenstechnik, Technical University of Munich, Munich, Germany, and CICECO/Departamento de Química, Universidade de Aveiro, 3810-193 Aveiro, Portugal

Liquid−liquid systems research increasingly concentrates on computer simulations. However, the possibility of adequately testing complex theoretical models against experiments is hindered by a lack of reliable reproducibility data for laboratory and pilot-plant measurements. This strongly limits meaningful evaluation of the increasingly complex process and equipment models/algorithms that are being developed. In this work, experimental data are obtained in a pilot-scale Kühni column, and model parameters and simulated data are generated using a drop population balance model and algorithm. The results can be summarized as follows: (i) As measured by the magnitude of careful random error and corresponding confidence limits estimates, the simulation results exhibit excellent agreement with experimental drop-size distributions and fair conformity with measured dispersed-phase hold-ups. (ii) Both experimental and simulated results show that interdrop coalescence is always present within a column extractor, even at low dispersed-phase hold-ups, and thus cannot be neglected in any physically realistic and accurate modeling.

Introduction

Many engineering processes involve the mixing of two immiscible liquids. An intimate interdispersion of the liquids is obviously of major importance for an efficient extraction operation, as the interfacial area available for mass transfer is thus significantly increased.

Thus, in the past few decades, mechanically agitated devices for liquid−liquid contact in extraction equipment have acquired great importance, because of their capability of creating and maintaining large interfacial areas, which promote mass transfer. Contrary to early theoretical expectation, however, the efficient behavior of these contactors has been shown to be due not only to these large interfacial areas, but also to the mixing effects caused by drop interactions, i.e., breakage and coalescence.

In recent years, many authors have spent considerable efforts in modeling these columns and in attempting experimental validation of their models. Models such as those of Cruz-Pinto;[1] Casamatta and Vogelpohl;[2] Laso et al.;[3] Tsouris et al.;[4] and, more recently, Gerstlauer et al.[5] have been declared able to describe the results of their authors' ad hoc experiments with reasonable accuracy, even if most of them adopted significant simplifications—such as ignoring coalescence and/or considering only the steady state—to make calculations feasible in a reasonable amount of time.

Recently, an algorithm previously developed by Ribeiro[6,7] has been modified to accurately describe the transient behavior of a continuous ideally agitated vessel, ignoring no important phenomena except Marangoni effects, that required only modest computer resources and very low computation times. Details of these models and corresponding algorithms are given elsewhere by Ribeiro et al.[8] This algorithm, further adapted by Regueiras[9,10] to model an agitated column by stagewise solution of the population balance equations under dynamic conditions was designed to compute the drop-size distribution and local dispersed-phase hold-up profiles along a column. Its use yielded encouraging qualitative agreement with the experimental results obtained in a pilot-plant Kühni column.[11]

On the other hand, a thorough search of all available relevant literature has shown that no quantitative studies of the error in the measurement of drop-size distributions and hold-up have ever been published. As mentioned above, several simulation models have been developed, but the various research groups involved apparently have never fully taken into consideration possible experimental errors when comparing simulated and experimental results. The objective of this paper is to report the results of an error analysis on such experimental measurements and to conclude how experimental errors affect and should guide theoretical model and algorithm evaluation studies. Because the hydrodynamics alone was contemplated, all experiments were conducted in the absence of mass transfer and so with no solute.

* To whom correspondence should be addressed. Address: Department of Chemistry, University of Aveiro, 3810-193 Aveiro, Portugal. Tel.: 00-351-234-370733/360. Fax: 00-351-234-3700084. E-Mail: cpinto@dq.ua.pt.

[†] CIEA/Departamento de Engenharia Química, Instituto Superior de Engenharia do Porto.

[‡] Faculdade de Engenharia, Instituto Superior de Engenharia do Porto.

[§] Technical University of Munich.

[||] Universidade de Aveiro.

10.1021/ie030277i CCC: $27.50
Published on Web 01/22/2004

Table 1. Physical Properties of Toluene and Water at 20 °C

	density ($kg \cdot m^{-3}$)	viscosity ($Pa \cdot s$)	interfacial tension ($N \cdot m^{-1}$)
toluene	866.7	0.586×10^{-3}	33.4×10^{-3}
water	998.2	1.003×10^{-3}	

Experimental Work

The experimental work was carried out by Gomes[11] in a Kühni pilot-plant column (inside diameter of 150 mm, active height of 2520 mm, divided into 36 stirred compartments with 25% free area baffle plates, located at Munich University). The test system was the equilibrated, standard, high-interfacial-tension toluene (dispersed phase)−water (continuous phase) system. The physical properties of both fluids (at 20 °C) are reported in Table 1.

Experiments were performed at room temperature, under steady-state conditions, and under both normal and extreme conditions of agitation intensity and dispersed- and continuous-phase flow rates. Details of the data reported by Gomes[11] can be obtained from the authors, and other similar data are available from Zamponi.[12]

The extraction column is equipped with measurement devices that allow the investigation of the hydrodynamic conditions along the column. A photoelectric technique, initially developed by Pilhofer,[13] was used to measure the axial drop-size distribution profiles. The drop slug length in a capillary was determined with two pairs of photoelectric cells on a calibrated capillary. This instrumentation was installed in five compartments (2nd, 5th, 11th, 21st, and 35th) of the column. For each measurement of the drop-size distribution, 1000 sample drops were collected. Unfortunately, the experimental setup did not provide for the acquisition of the feed drop-size distribution, nor even of the drop-size distribution at the first column stage.

Some difficulties were found during the calibration of the probe located at the fifth stage. Later, the results of the measurements confirmed the anomalous behavior of the measuring device at this stage, possibly due to a defective probe.

The local hold-ups were monitored at four compartments, namely, the 4th, 10th, 16th, and 22nd, using a noninvasive ultrasonic technique described by Yi and Tavlarides.[14] Simultaneously, the overall column hold-up was measured using the pressure difference between the top and bottom of the active part of the column. All of these data, as well as the intensity of agitation and the flow rates of the dispersed and continuous phases, were recorded on-line using a personal computer.

Experimental results were obtained as data files created by Hydromess,[13] a computer program developed at the University of Clausthal (Clausthal, Germany) and implemented in the University of Munich's pilot-scale Kühni column. From a collection of 1000 drop-size measures, this program computes the number, volume, and surface-area drop-size distributions and the mean diameters. Drop-size distributions were obtained for steady-state conditions alone, with each measurement taking about 2 h, depending on the agitation intensities and the resulting average drop size. In addition, because different runs were performed under the same operating conditions but under uncontrolled environmental conditions (in particular, environment temperature was not even measured), these are also liable to variation.

Although uncontrolled environmental conditions could be expected to be an important source of variation of the size and hold-up measured data, no significant difference was observed between measurements in two experimental campaigns at different times of the year.

Several experiments were planned and performed, under steady state and at a constant continuous-phase/dispersed-phase flow ratio ($Q_C/Q_D = 1.28$). The standard operating conditions were defined for two different sets of fluid flow velocities labeled as follows:

B12: $Q_D = 120\ L \cdot h^{-1}$, $Q_C = 94\ L \cdot h^{-1}$, agitation rate = 170 rpm

B16: $Q_D = 160\ L \cdot h^{-1}$, $Q_C = 125\ L \cdot h^{-1}$, agitation rate = 140 rpm

Error Analysis

During the experiments carried out with the extraction column, we detected evidence of systematic errors affecting the drop-size measurements in the fifth stage. Unfortunately, it was impossible to identify and correct the source of these possible errors. The random errors, however, whose magnitude is crucial to data quality, cannot be avoided but can be the object of adequate statistical treatment.

Statistical theory allows us to determine a confidence interval for the most plausible estimate—the sample average, $\bar{x}$—of the mean, μ, of a population and to state with some predefined plausibility that the sought mean will lie somewhere within such an interval.

In our case, small-sample theory must be invoked for this purpose, and the confidence interval can be calculated as $\bar{x} \pm ts/\sqrt{n}$, where s is the sample mean square deviation, n is the number of available samples, and t is the Student's t for the appropriate significance level (98%, in our case) and number of degrees of freedom ($n - 2$, because two of degrees of freedom used to estimate the mean and the mean square deviation).

Confidence Channel for Local Drop-Size Distributions

Under normal industrial or pilot-plant experimental conditions, the drop-size distribution is influenced by fluid contamination through variations in the interfacial tension, a key variable affecting the drop interaction dynamics. It is almost impossible and highly uneconomical to stop an industrial installation to perform fluid cleansing, although periodic removal of impurities accumulated at the top or bottom interfaces can be adopted as routine procedure. Further, interfacial tension is highly dependent on temperature, an environmental variable whose control is highly unwieldy to implement.

As stated above, in the experimental setup used here, environmental conditions were neither controlled nor measured, so we planned repeat runs to study data reproducibility and the resulting measurement and sampling errors. This information was used to realistically assess the quality of the theoretical performance predictions.

The absolute instrumental error implicit in the size class-by-class drop counts directly influences the relative drop-size errors, because drops might be reported to belong to one class when they should be reported to belong to a neighboring one. Figure 1 shows the relative

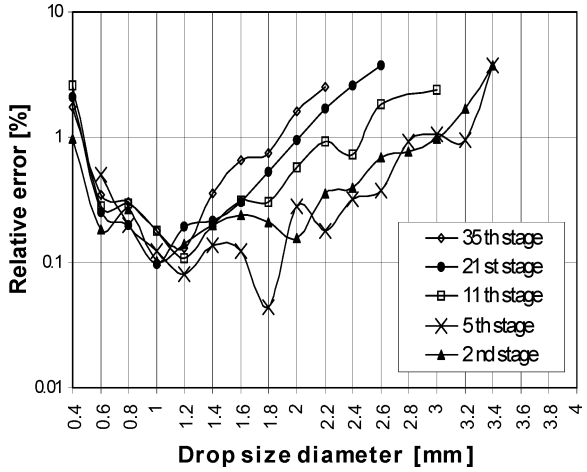

Figure 1. Relative error calculated from number drop-size distributions at different stages of the column under B16-standard operating conditions (Q_C = 125 L·h^{-1}, Q_D = 160 L·h^{-1}, 140 rpm).

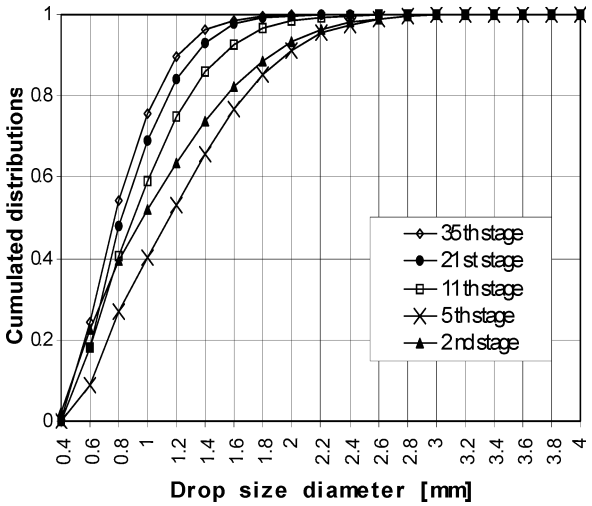

Figure 2. Cumulative frequencies for the number drop-size distributions at the different stages of the column under B16-standard operating conditions (Q_C = 125 L·h^{-1}, Q_D = 160 L·h^{-1}, 140 rpm).

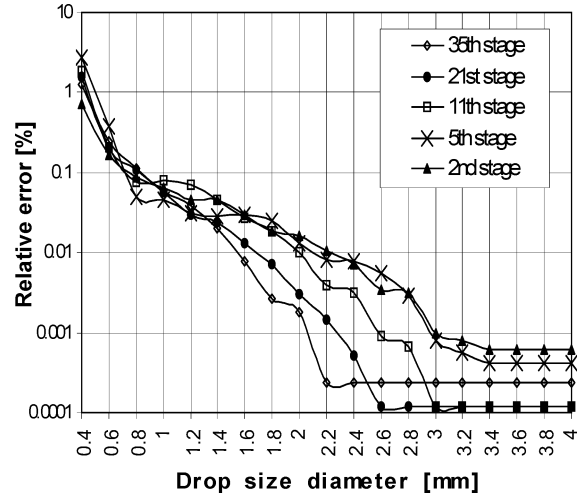

Figure 3. Relative error calculated from cumulative number drop-size distributions at the different stages of the column under B16-standard operating conditions (Q_C = 125 L·h^{-1}, Q_D = 160 L·h^{-1}, 140 rpm).

error, $ts/(\bar{x}\sqrt{n})$, as computed by the Student's *t*-distribution for six runs performed under the operating conditions designated B16-standard condition; the curves are typically U-shaped, with both small and large size classes exhibiting anomalously high relative errors.

For small drop sizes, this anomaly can be ascribed to small-diameter drops not being stretched enough by the capillary, thus presenting insufficient length to be accurately measured. The fact that the error is minimal for drop diameters just above the capillary diameter (0.8 mm) seems to confirm this interpretation.

In the case of the larger sizes, which are relatively infrequent in number, the sampling error is correspondingly high because even only one misplacement error can translate into a large relative error. This interpretation seems to be confirmed by the error in the larger sizes (Figure 1) increasing upward along the column, the direction along which, for the present conditions, the tail of the number size distribution becomes shallower and shallower.[11]

To minimize the relative error for the larger size classes, we took the cumulative size distributions. Using the cumulative frequencies (i.e., counting for each class all drops smaller than the upper limiting size of the class), the error curves become significantly different, because the larger size classes now contain a considerably larger number of drops.

Figure 2 shows the average cumulative frequencies at the different column stages for the B16-standard experiment. The following features should be noted in this figure: (i) No sizes under 0.4 mm are measured. (ii) The position of the cumulative curve for the second stage is anomalous (with the cumulative frequencies lying above those of the fifth stage, although they should be below); this anomaly can be ascribed either to perturbations resulting from the closeness of the feed stage or to systematic error (which is not eliminated by averaging) in the size measurement at the fifth stage, as implied by the particular difficulty in the calibration of the corresponding capillary. (iii) The rise of the cumulative curves becomes gradually steeper for successively higher stages of the column, confirming the dominance of division over coalescence in this range of agitation power densities, as found by virtually all previous research.

Figure 3 shows the estimated (random) relative error of the cumulative frequencies, computed from the Student's *t*-distribution for different runs at B16-standard conditions. A careful analysis of this plot shows the following characteristics: (i) very high relative errors for the smaller size classes (0.4 and 0.6 mm), probably due to class confusion (insufficient accuracy) by the measuring device; (ii) plausible relative errors (below 7%) for the size classes immediately above the capillary diameter (0.8 mm); and (iii) diminishing errors for the successively coarser classes, as expected from the regularization effect of using cumulative drop numbers.

The same study was performed for the results of B12-standard runs. Under these operating conditions, the average drop size obtained in the first two column stages is larger. This fact results from the increase in the coalescence frequency brought about by the higher rotation rate, combined with the lower flows, as can be seen in Figure 4, which shows experimental local drop-size number distributions along the column height under B16- and B12-standard conditions. It should also be noticed in Figure 4 that the B12-standard conditions

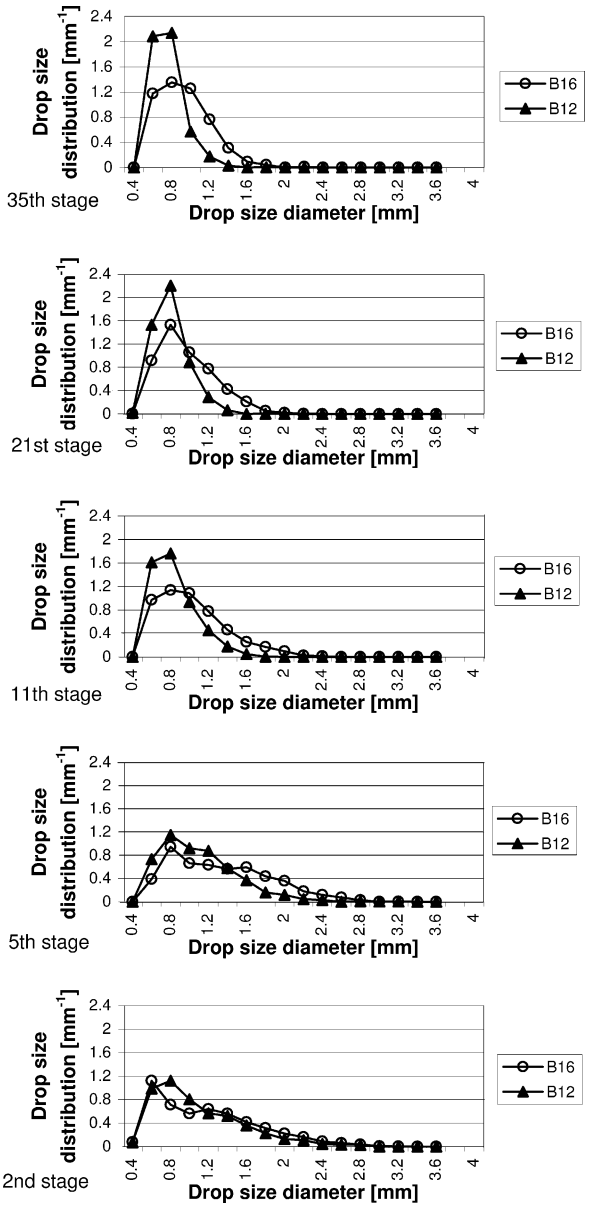

Figure 4. Drop-size number distributions at the different stages of the column under B12-standard (Q_C = 94 L·h^{-1}, Q_D = 120 L·h^{-1}, 170 rpm) and B16-standard (Q_C = 125 L·h^{-1}, Q_D = 160 L·h^{-1}, 140 rpm) operating conditions.

expectedly lead to a higher breakage frequency at the upper stages of the column than the B16-standard conditions.

Under these new operating conditions, however, the errors for the large drop sizes are slightly smaller than under B16-standard conditions,with Figure 5 showing the same general behavior of the relative error of the number drop-size distributions.

As before, to decrease the relative error of the larger drop-size frequencies in the upper stages, cumulative distributions were computed.

Figure 6 presents a comparison among the average cumulative drop-size distributions measured at the different column stages under B12-standard conditions. The anomalous position of the curve for the fifth stage, although less marked than for the B16-standard conditions, should again be noted. In Figure 7, except for drop sizes smaller than the capillary diameter (0.8 mm), all (random) errors are smaller than 7%, which is quite

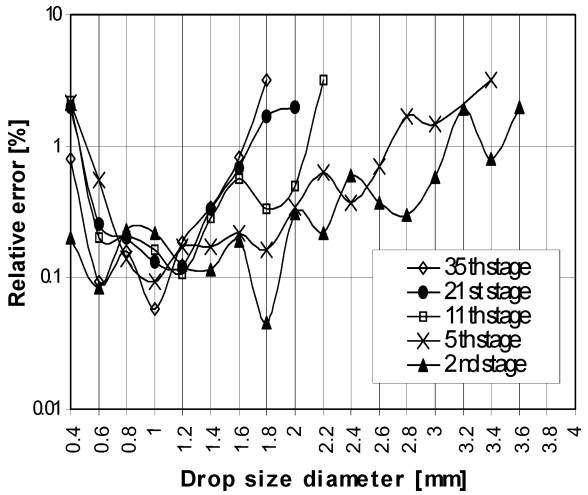

Figure 5. Relative error of number drop-size distributions at the different stages of the column under B12-standard operating conditions (Q_C = 94 L·h^{-1}, Q_D = 120 L·h^{-1}, 170 rpm).

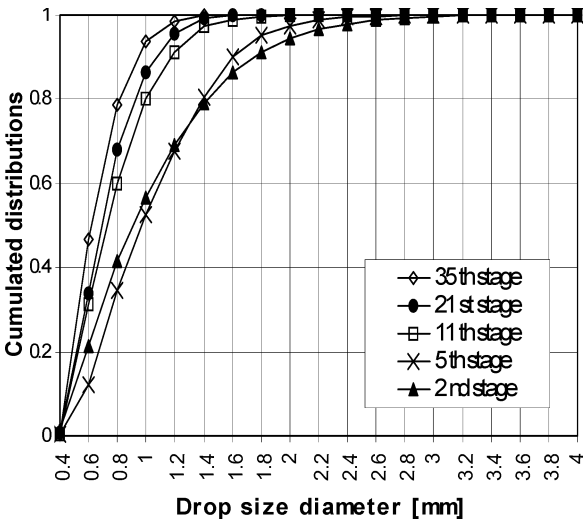

Figure 6. Cumulative frequencies for the number drop-size distributions at the different stages of the column under B12-standard operating conditions (Q_C = 94 L·h^{-1}, Q_D = 120 L·h^{-1}, 170 rpm).

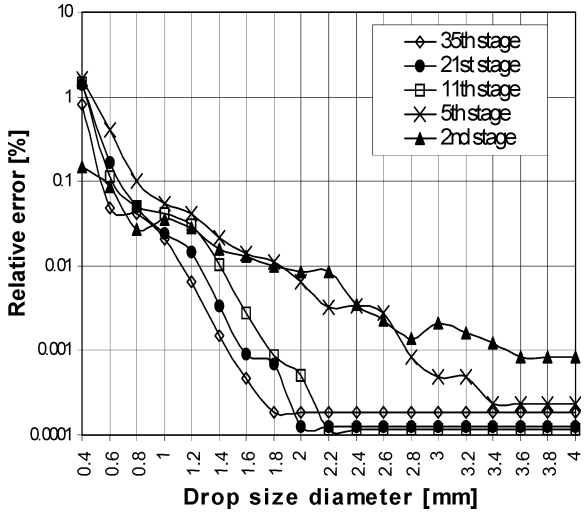

Figure 7. Estimate of the relative error of the number drop-size distributions for the different stages of the column under B12-standard operating conditions (Q_C = 94 L·h^{-1}, Q_D = 120 L·h^{-1}, 170 rpm).

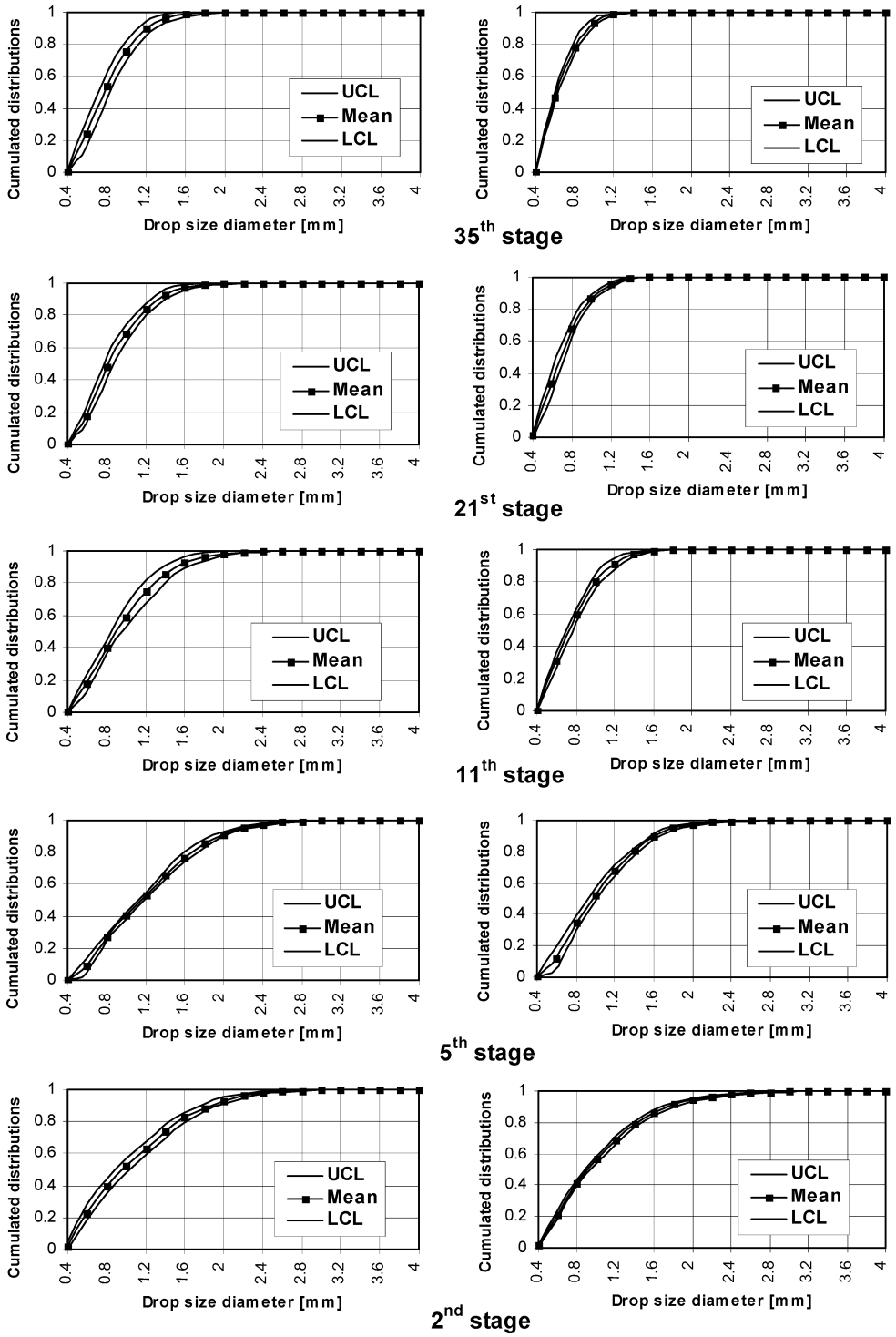

Figure 8. Experimental cumulative drop-size distributions, together with the confidence limits. Standard operating conditions: (left) B16 (Q_D = 160 L·h^{-1}, Q_C = 125 L·h^{-1}, 140 rpm), (right) B12 (Q_D = 120 L·h^{-1}, Q_C = 94 L·h^{-1}, 170 rpm); UCL = upper (98%) confidence limit, mean = average, LCL = lower (98%) confidence limit.

satisfactory and similar to the values obtained for the B16-standard conditions (compare Figures 3 and 7).

Figure 8 summarizes the average cumulative frequencies and the corresponding confidence channels (Student's *t*, 98%) at the different column stages for standard B16 and B12 operating conditions. Similar reproducibility data have not previously been published for column pilot-plant experiments, and as discussed below, such data are of paramount importance in theoretical model and simulation algorithm evaluation.

Confidence Channel for Local Dispersed-Phase Hold-Ups

The relative errors for the local hold-ups were similarly calculated by means of the Student's *t*-distribution over 30 different experiments under B16-standard conditions and over 21 different experiments under B12-standard conditions. All experiments were performed under uncontrolled environmental conditions (temperature, interface fouling, etc.).

Because the ultrasound calibration[11] was performed

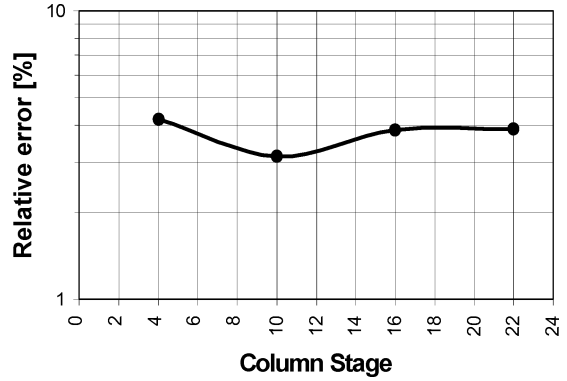

Figure 9. Relative error for the local dispersed-phase hold-up profile under B16-standard operating conditions (Q_C = 125 L·h^{-1}, Q_D = 160 L·h^{-1}, 140 rpm).

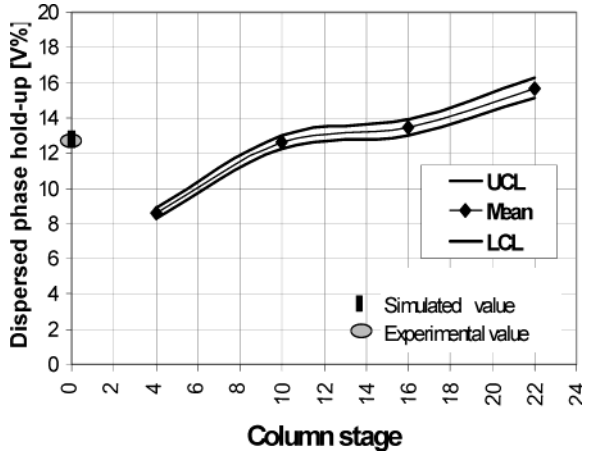

Figure 10. Confidence channel for the dispersed-phase hold-up measured profile under B16-standard operating conditions (Q_C = 125 L·h^{-1}, Q_D = 160 L·h^{-1}, 140 rpm); UCL = upper (98%) confidence limit, mean = average, LCL = lower (98%) confidence limit. The experimental and simulated overall dispersed-phase hold-ups are represented as those of column stage 0.

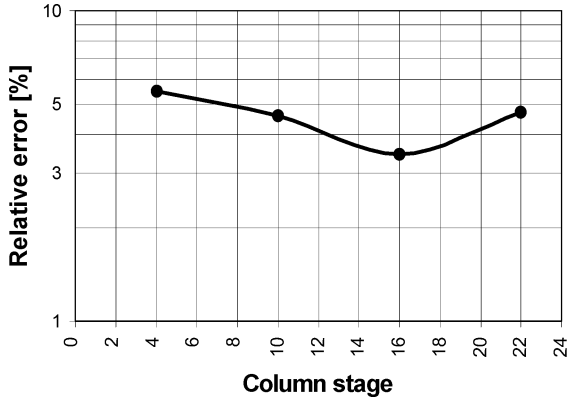

Figure 11. Relative error for the local dispersed-phase hold-up profile under B12-standard operating conditions (Q_C = 94 L·h^{-1}, Q_D = 120 L·h^{-1}, 170 rpm).

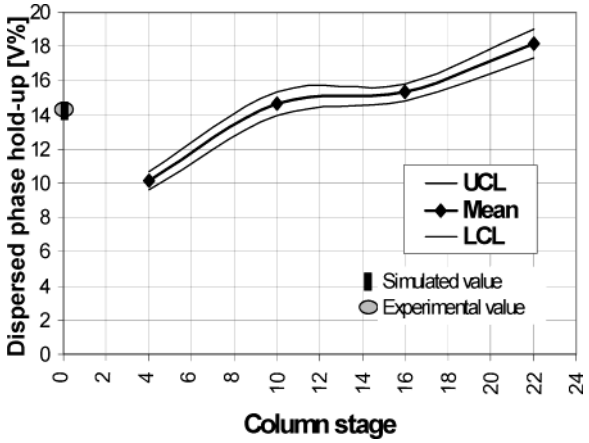

Figure 12. Confidence channel for the dispersed-phase hold-up measured profile under B12-standard operating conditions (Q_C = 94 L·h^{-1}, Q_D = 120 L·h^{-1}, 170 rpm); UCL = upper (98%) confidence limit, mean = average, LCL = lower (98%) confidence limit. The experimental and simulated overall dispersed-phase hold-ups are represented as those of column stage 0.

only once a day, day-long temperature variations might significantly influence interfacial tension and, consequently mean drop size, which affects the ultrasound readings.

The relative errors for the hold-up measurements under B16-standard conditions are shown in Figure 9, where it can be noticed that they are consistently ca. 4%. This is remarkable, given that mean drop sizes and temperature are bound to vary significantly along column height.

The confidence channel that was used as a standard for the comparison of model predictions to actual measurements is shown in Figure 10.

For the 21 experiments under B12-standard operating conditions, similar results were obtained, as exhibited in Figures 11 and 12.

It should be further noticed that B12 conditions are noticeably outside current industrial practice and were tested with a view to the application of the model to predictive control under large operating disturbances. Such anomalous conditions might, however, be transiently important, for instance, when, to prevent column flooding, both fluid flows are reduced while flow ratio is maintained.

Confidence Intervals for Overall Column Hold-Ups

Local and overall hold-up data were simultaneously collected. The relative (random) error for the overall hold-up of the column was estimated as 2.30% for the B16-standard operating conditions and as 2.17% for B12-standard operating conditions.

As can be seen in Figures 10 and 12, the simulated values for overall hold-up obtained for B16-and B12-standard operating conditions, respectively, show a satisfactory agreement with the experimental values, demonstrating different sensitivities for the ultrasonic and pressure techniques

Confidence Intervals and Model Parameter Estimation

The algorithms for the solution of the population balance equations (PBEs) under dynamic conditions, designed to obtain the drop-size distribution and dispersed-phase hold-up profiles along the column height while accounting for drop breakage and coalescence, are very complex and computationally demanding, given the multiple stages in the column (each approximately

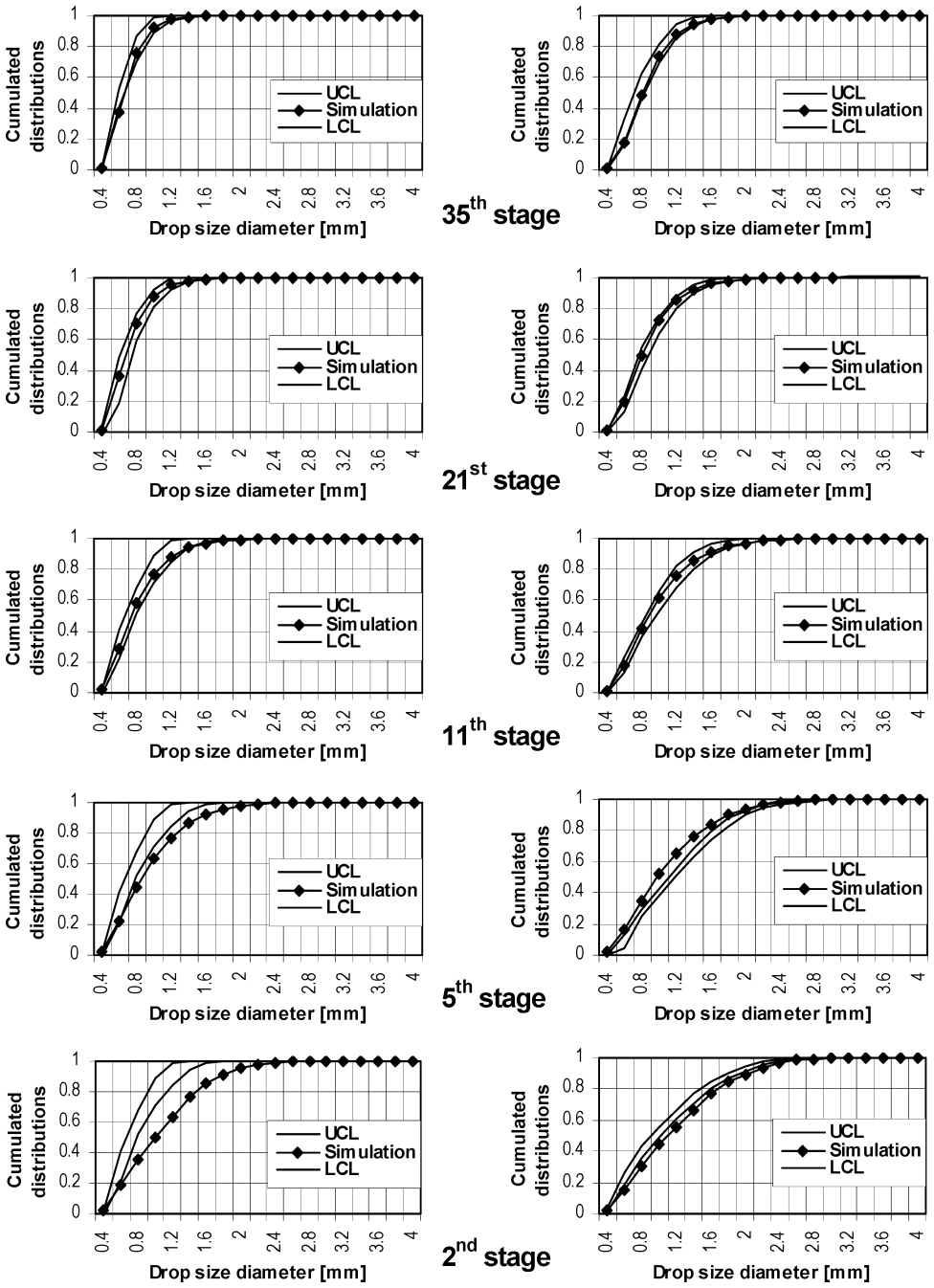

Figure 13. Simulated values of drop-size distributions, together with confidence limits. Standard operating conditions: (left) B12 (Q_D = 120 L·h^{-1}, Q_C = 94 L·h^{-1}, 170 rpm), (right) B16 (Q_D = 160 L·h^{-1}, Q_C = 125 L·h^{-1}, 140 rpm); UCL = upper (98%) confidence limit, mean = average, LCL = lower (98%) confidence limit.

describable as an ideally agitated vessel) and the corresponding interstage flows.

The proposed model and parameter optimization algorithm[15] combine the following two components:

(a) The first component is the drop interaction model developed by Coulaloglou and Tavlarides[16] as solved by Ribeiro,[6] with its well-known four interaction parameters, namely, (a1) two parameters (k_{1Break} and k_{2Break}) for the breakage frequency

$$g(d) = k_{1Break}\frac{\epsilon^{1/3}}{(1+\phi)d^{2/3}}\exp\left[-k_{2Break}\frac{\sigma(1+\phi)^2}{\rho_D d^{5/3}\epsilon^{2/3}}\right] \quad (1)$$

where the daughter drop-size distribution is normal, with the mean volume equal to one-half the mean volume of the parent drop, and (a2) two parameters (k_{1Coal} and k_{2Coal}) for the coalescence frequency

$$c(d,d') = h(d,d')\,\lambda(d,d') \quad (2)$$

where

$$h(d,d') = k_{1Coal}\frac{\epsilon^{1/3}}{1+\phi}(d^2 + d'^2)(d^{2/3} + d'^{2/3})^{1/2} \quad (3)$$

is the collision frequency and

$$\lambda(d,d') = \exp\left[-k_{2Coal}\frac{\rho_C\mu_C\epsilon}{\sigma^2(1+\phi)^3}\left(\frac{dd'}{d+d'}\right)^4\right] \quad (4)$$

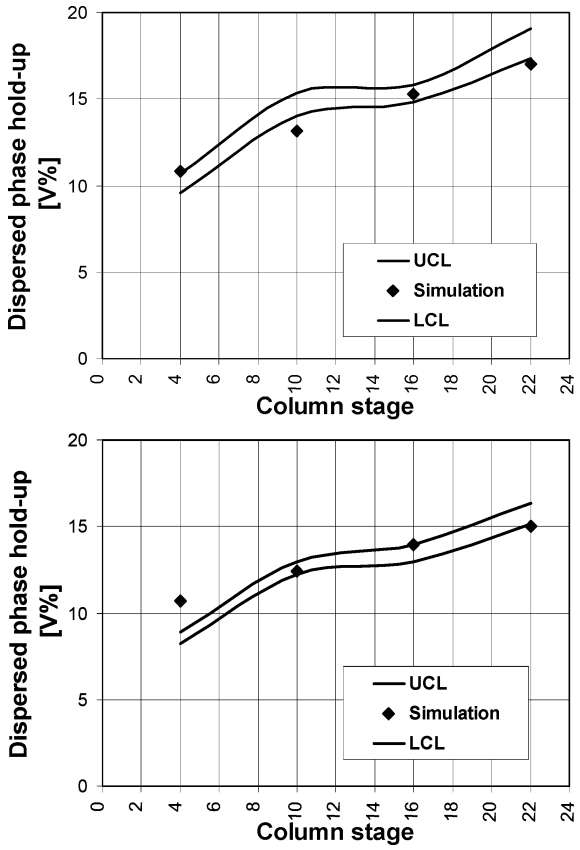

Figure 14. Simulated values of local dispersed-phase hold-up profile, together with confidence limits. Standard operating conditions: (left) B12 (Q_D = 120 L·h^{-1}, Q_C = 94 L·h^{-1}, 170 rpm), (right) B16 (Q_D = 160 L·h^{-1}, Q_C = 125 L·h^{-1}, 140 rpm); UCL = UCL = upper (98%) confidence limit, mean = average, LCL = lower (98%) confidence limit.

is the collision coalescence efficiency.

(b) The second component is an original phase interstage transport model developed by Regueiras,[9,10] with three additional transport parameters, namely, (b1) one parameter ($k_{1PowerFact}$) for the agitation speed−power density

$$\epsilon = \frac{4P(k_{1PowerFact})^3}{\pi {D_C}^2 H[\rho_C(1-\phi)+\rho_D\phi]} \tag{5}$$

where the power input, P, to each column compartment is

$$P = N_P N^3 {D_R}^5 \rho_C \tag{6}$$

and the power number, N_P, is given by the correlation obtained by Fischer in Kumar and Hartland[17]

$$N_P = 1.08 + \frac{10.94}{{Re_R}^{0.5}} + \frac{257.37}{{Re_R}^{1.5}} \tag{7}$$

(b2) one parameter ($k_{1Transport}$) for the effective flow area in interstage constrictions

$$C_R = (1 - k_{1Transport})e + k_{1Transport} \tag{8}$$

where e is the fractional free area, according to Goldman;[18] and (b3) one parameter ($k_{2Transport}$) for modeling the size-dependent axial dispersion (i.e., the effect of a random variation of the drop velocities), where the random component of the drop velocity is assumed to be isotropic and to have an average magnitude described by Regueiras[9] as a fraction of the velocity of the impeller tip

$$v_D = k_{2Transport} N D_R \pi \tag{9}$$

The axial slip velocity (drop velocity relative to the continuous phase) in each size class is then modified by summing or subtracting the average value of the axial projection of this random component, and the number fraction of drops of each class that pass from one compartment to each of its neighbors is computed accordingly. This is merely a more general formulation of axial dispersion than the one suggested by Tsouris.[19]

In the absence of direct experimental measurements at the dispersed-phase distributor outlet, an average value and a standard deviation of the feed drop diameter distribution were considered and were iteratively adjusted[11] together with the seven intrinsic model parameters. The feed drop diameter distribution is assumed to be log−normal. In fact, preliminary runs showed that, among various distribution types, this is the most adequate one for describing our data.

The optimization algorithm selected was Levenberg−Marquardt's, for its recognized capability of handling highly multidimensional spaces and its economy on function calls, in cases where the objective function deviates significantly, even close to a minimum, from quadratic behavior—the ideal for second-order methods. The objective function was defined as a weighted sum of the squared deviations between the calculated and experimental values of the overall and local dispersed-phase hold-ups and of the local cumulative, number-based drop-size distributions.

The implementation adopted was that due to Nash,[20] written by Regueiras,[10] which uses double precision (64 bits, with 1 for the sign, 11 for the exponent, and 52 for the mantissa; range of $\pm 1.7 \times 10^{308}$ with at least 15 digits of precision) in all critical number representations and is especially careful in the estimate of the objective function derivatives. Separate reports will more fully describe and discuss these computations and their results.

As can be seen in Figures 13 and 14, the simulated cumulative drop-size distributions and local hold-up profiles globally fall within the experimental confidence limits.

The most important exceptions occurred at the second stage (which is heavily influenced by the unknown feed conditions) and the fifth stage (where we suspect systematic errors due to deficiencies in the column instrumentation). Thus, we obtained reliable evidence that the computed residuals are consistent with the experimental errors.

This same methodology, whereby the experimental errors are adequately quantified and made to influence the search for optimized model solutions, is now part of our routine model and algorithm evaluations and is recommended for any similar future work.

Using these procedures, we are already currently able to provide encouragingly good fits of PBE model solutions to experimental pilot-plant column data and have obtained clear indications that interdrop coalescence cannot be neglected, even for steady-state liquid−liquid systems with low dispersed-phase hold-ups. This challenges somewhat the approaches and assumptions adopted in many oversimplified studies,[5] but is indeed

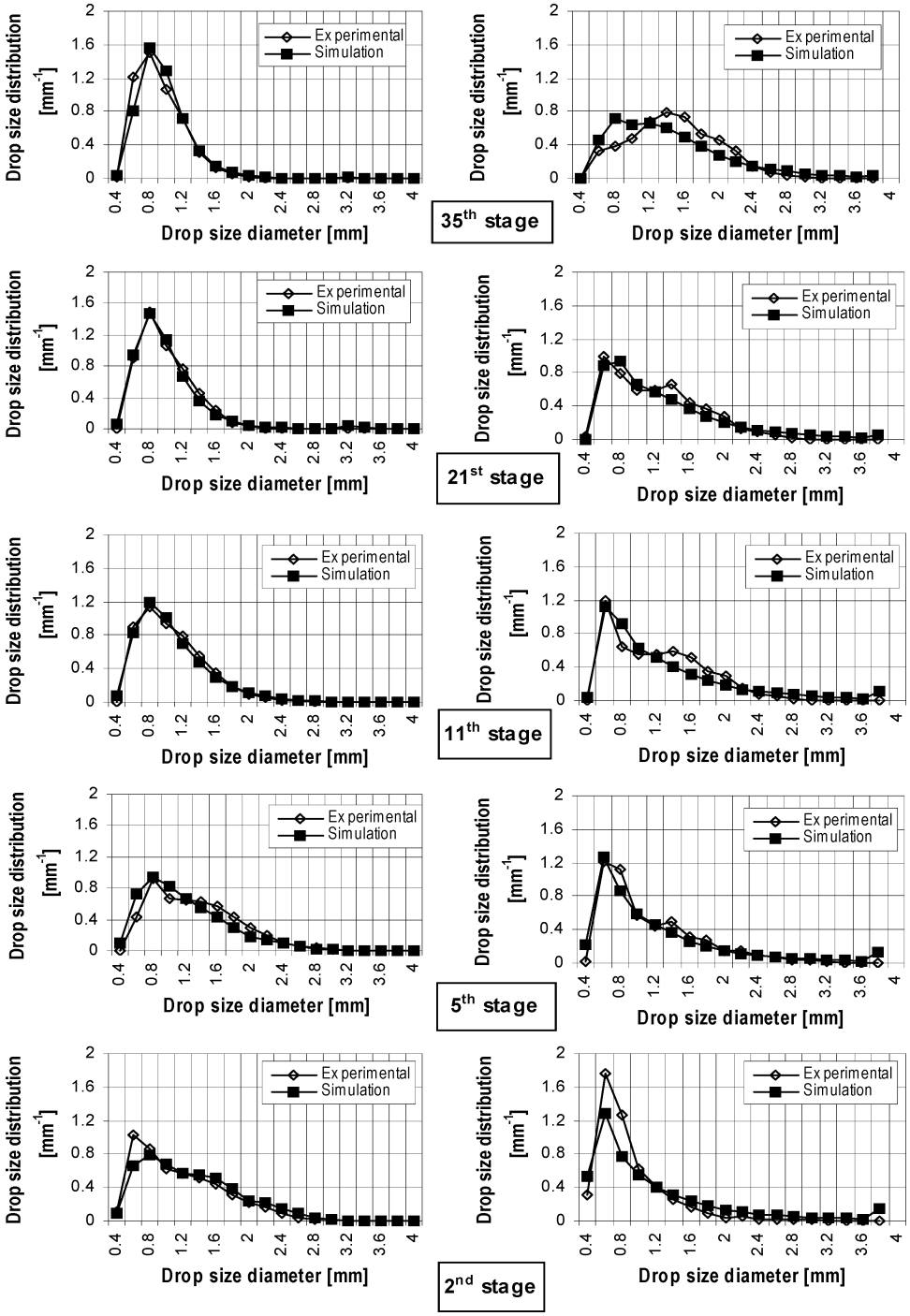

Figure 15. Simulated and experimental values of number drop-size distributions. (left) B16-standard conditions (Q_D = 160 L·h^{-1}, Q_C = 125 L·h^{-1}, 140 rpm), (right) B16 (Q_D = 160 L·h^{-1}, Q_C = 125 L·h^{-1}, 100 rpm).

what is to be physically expected, as no strict steady-state hydrodynamic equilibrium could ever be reached under batch conditions without competing drop breakage and coalescence.

To fully document this behavior, we explored normal-agitation as well as low-agitation column operating conditions,[11] to further intensify coalescence, with the results shown in Figure 15. At the lowest agitation speed, a marked effect of coalescence can be identified, even in the upper stages of the column.

The larger drops obtained overall, and the corresponding larger drop diameters at the upper stages, are justified (and can be approximately predicted by the algorithm) by the increased coalescence relative to breakage, combined with the more rapid motion of such large drops up along the column. The poorest agreement between simulated and experimental drop-size distributions was obtained at the lowest instrumented stage (second) of the column (also the closest to the inlet dispersed-phase distributor, for which experimental drop-size data could not be measured, thus having to be crudely estimated).

Additionally, it can be noted that, at 100 rpm, drop coalescence combined with less intensive breakage is responsible for the bimodal shape of the drop-size distributions (as predicted by the model), which dies out only at the highest stages of the column, whereas the distributions are unimodal at 140 rpm, except at the lowest stages.

Conclusions

Statistical studies have been performed on the random errors associated with drop size and local hold-up measured data in an agitated pilot-scale liquid−liquid extraction column.

The results of these studies show that confidence intervals for these measurements are very important tools for the evaluation and interpretation of model fitting and simulation results.

Experiments over a broad spectrum of operating conditions showed that steady-state drop-size distributions result from equilibria between breakage and coalescence processes (in addition to flow processes in continuous operations), so that, despite their computational burden, such processes cannot be neglected when modeling the behavior of agitated liquid−liquid dispersions.

Acknowledgment

This work was carried out under the gratefully acknowledged financial supports of the INIDA Cooperation Program (JNICT/DAAD) and IPP−Fundo de Apoio à Investigação. Cooperation from Professor J. Stichlmair and his staff at the Technical University of Munich is also gratefully acknowledged.

Nomenclature

C_R = constriction factor
d, d' = drop diameter, m
D_C = internal column diameter, m
D_R = rotor diameter, m
e = fractional free cross-sectional area (S_e/S)
$g(d)$ = drop breakage frequency, s^{-1}
$h(d,d')$ = drop collision frequency, s^{-1}
H = compartment height, m
k_{1Break}, k_{2Break} = breakage constants
k_{1Coal} = coalescence constant, m^{-3}
k_{2Coal} = coalescence constant, m^{-2}
$k_{1PowerFact}$ = parameter for the agitation speed−power
$k_{1Transport}$ = parameter for the effective flow area
$k_{2Transport}$ = parameter for the axial dispersion
N = rotor speed, rev s^{-1}
N_P = power number, dimensionless
P = power input per compartment, W
Re_R = rotor Reynolds number ($ND_R^2\rho_C/\mu_C$)
S = column cross sectional area, m^2
v_D = radial velocity of the continuous phase, m s^{-1}

Greek Symbols

ϵ = mechanical power dissipation per unit mass, W kg^{-1}
$\lambda(d,d')$ = coalescence efficiency, dimensionless
μ_C = continuous-phase viscosity, Pa s
π = 3.1416
ρ_C = continuous-phase density, kg m^{-3}
ρ_D = dispersed-phase density, kg m^{-3}
σ = interfacial tension, N m^{-1}
ϕ = dispersed-phase hold-up

Subscripts

C = continuous phase
D = dispersed phase

Literature Cited

(1) Cruz-Pinto, J. J. C. Experimental and Theoretical Modelling Studies of the Hydrodynamic and Mass Transfer Processes in Countercurrent-Flow Liquid−Liquid Extraction Columns. Ph.D. Dissertation, The Victoria University of Manchester, Manchester, U.K., 1979.

(2) Casamatta, G.; Vogelpohl, A. Modelling of Fluid Dynamics and Mass Transfer in Extraction Columns. *Ger. Chem. Eng.* **1985**, *8*, 96.

(3) Laso, M.; Steiner, L.; Hartland, S. Dynamic Simulation of Liquid−Liquid Agitated Dispersions—I. Derivation of a Simplified Model. *Chem. Eng. Sci.* **1987**, *42*, 2429.

(4) Tsouris, C.; Kirou, V. I.; Tavlarides, L. L. Breakage and Coalescence Models for Drops in Turbulent Dispersions. *AIChE J.* **1994**, *40*, 395.

(5) Gerstlauer, A.; Mitrovic, A.; Gilles, E. D.; Zamponi, G.; Stichlmair, J. A Detailed Population Model for the Dynamics of Agitated Liquid−Liquid Dispersions. In *Value Adding through Solvent Extraction*; Shallcross, D. C., Paimin, R., Prvcic, L. M., Eds.; University of Melbourne: Melbourne, Australia, 1996.

(6) Ribeiro L. M. Simulação Dinâmica de sistemas líquido−líquido. Ph.D. Dissertation, Universidade do Minho, Braga, Portugal, 1995.

(7) Regueiras, P. F. R.; Ribeiro, L. M.; Guimarães, M. M. L.; Cruz-Pinto, J. J. C. Precise and Fast Computer Simulations of the Dynamic Mass Transfer behaviour of Liquid−Liquid Agitated Contactors. In *Value Adding through Solvent Extraction*; Shallcross, D. C.; Paimin, R.; Prvcic, L. M., Eds.; University of Melbourne: Melbourne, Australia, 1996.

(8) Ribeiro, L. M.; Regueiras, P. F. R.; Guimarães, M. M. L.; Cruz-Pinto, J. J. C. Numerical Simulation of Liquid−Liquid Agitated Dispersions on the VAX 6520/VP. *Comput. Syst. Eng.* **1995**, *6*, 465.

(9) JNICT/FCT−Projecto−Jovens Doutorados, Faculdade de Engenharia da Universidade do Porto, Porto, Portugal. Unpublished results, 1999.

(10) Regueiras, P. F. R.; Gomes, M. L.; Ribeiro, L. M., Guimarães, M. M. L., Cruz-Pinto, J. J. C. Efficient Computer Simulation of The Dynamics of An Agitated Liquid−Liquid Extraction Column. In *CHEMPOR'98−7th International Chemical Engineering Conference*; Ramôa Ribeiro, F., Alves, S. S., Eds.; Instituto Superior Técnico: Lisboa, Portugal, 1998; p 765.

(11) Gomes, M. L. A. C. N. Comportamento Hidrodinâmico de Colunas Agitadas de Extracção Líquido-Líquido. Ph.D. Dissertation, Universidade do Minho, Braga, Portugal, 1999.

(12) Zamponi, G. Das dynamische Verhalten einer gerührten Solventeextraktionskollonne. Ph.D. Dissertation, Technische Universität München, München, Germany, 1996.

(13) Genenger, B.; Lohrengel, B.; Lorenz, M.; Vogelpohl, A. Hydromess- *Messsystem zur Bestimmung der Blasen−und Tropfengrösse in Mehrphasenströmungen*; Institut für Thermische Verfahrenstechnik der TU Clausthal: Clausthal, Germany, 1991.

(14) Yi, J.; Tavlarides, L. L. Model for hold-up measurements in liquid dispersions using an ultrasonic technique. *Ind. Eng. Chem. Res.* **1990**, *29*, 475.

(15) Ribeiro, L. M.; Regueiras, P. F. R.; Guimarães, M. M. L.; Cruz-Pinto, J. J. C. Efficient algorithms for the dynamic simulation of agitated liquid−liquid contactors. *Adv. Eng. Software* **2000**, *31*, 985.

(16) Coulaloglou, C. A.; Tavlarides, L. L. Description of Interaction Processes in Agitated Liquid−Liquid Dispersions. *Chem. Eng. Sci.* **1977**, *32*, 1289.

(17) Kumar, A.; Hartland, S. A Unified Correlation for the Prediction of Dispersed-Phase Hold-Up in Liquid−Liquid Extraction Columns. *Ind. Eng. Chem. Res.* **1995**, 34, 3925.

(18) Goldmann, G. Ermittlung und Interpretation von Kennlinienfelderen einer gerührten Extraktionskolonne. Ph.D. Dissertation, Technische Universität München, München, Germany, 1986.

(19) Tsouris, C. Modelling and control of extraction columns. Ph.D. Dissertation, Syracuse University, Syracuse, NY, 1992.

(20) Nash, J. C. *Compact Numerical Methods for Computers: Linear Algebra and Function Minimisation*; Adam Hilger: Bristol, U.K., 1979.

Received for review April 2, 2003
Revised manuscript received October 15, 2003
Accepted December 5, 2003

IE030277I